RESEARCH ARTICLE | JULY 08 2025

# Infrared spectroscopic characterization of two types of products $HSiOH(H_2O)_n$ and $SiOH(H_2O)_n$ (n = 1-3) in the silicon–water reactions $\odot$

Wenhui Yan <sup>⑤</sup> ; Shuai Jiang; Shangdong Li; Jianxing Zhuang <sup>⑤</sup> ; Ailin Wang; Hua Xie <sup>⑥</sup> ; Gang Li <sup>Ѕ</sup> <sup>⑤</sup> ; Ling Jiang <sup>Ѕ</sup> <sup>⑥</sup>



J. Chem. Phys. 163, 024311 (2025) https://doi.org/10.1063/5.0280490





# Articles You May Be Interested In

Hydroxysilylene (HSi-OH) in the gas phase

J. Chem. Phys. (January 2025)

A global ab initio potential energy surface for the  $X^2A$  ground state of the Si + OH  $\rightarrow$  SiO + H reaction

J. Chem. Phys. (November 2013)

Theoretical predictions of properties and volatility of chlorides and oxychlorides of group-4 elements. II. Adsorption of tetrachlorides and oxydichlorides of Zr, Hf, and Rf on neutral and modified surfaces

J. Chem. Phys. (August 2014)



**The Journal of Chemical Physics** 

Special Topics Open for Submissions

**Learn More** 



# Infrared spectroscopic characterization of two types of products $HSiOH(H_2O)_n$ and $SiOH(H_2O)_n$ (n = 1-3) in the silicon-water reactions

Cite as: J. Chem. Phys. 163, 024311 (2025); doi: 10.1063/5.0280490 Submitted: 12 May 2025 • Accepted: 10 June 2025 •







Published Online: 8 July 2025

Wenhui Yan,<sup>1,2</sup> Shuai Jiang,<sup>1,2</sup> Shangdong Li,<sup>1,2</sup> Jianxing Zhuang,<sup>1,2</sup> Ailin Wang,<sup>1,2</sup> Hua Xie.<sup>1,2</sup> Gang Li,<sup>1,2,3</sup> and Ling Jiang<sup>1,2,3,3</sup>

# **AFFILIATIONS**

- <sup>1</sup> State Key Laboratory of Chemical Reaction Dynamics and Dalian Coherent Light Source, Dalian Institute of Chemical Physics, Chinese Academy of Sciences, Dalian 116023, China
- <sup>2</sup>University of Chinese Academy of Sciences, Beijing 100049, China

# **ABSTRACT**

The Si-O-H containing complexes are key interstellar species, but their structural characterization has been proven to be a challenging experimental target because of the difficulty in size selection of neutral clusters in general. Here, two series of products with the chemical formula of  $SiO_nH_{2n}$  and  $SiO_nH_{2n-1}$  (n=2-4) were prepared via the reactions of laser-ablated silicon atoms with the water molecules and characterized by using size-specific infrared-vacuum ultraviolet (IR-VUV) spectroscopy and quantum chemical calculations. The  $SiO_nH_{2n}$  and  $SiO_nH_{2n-1}$  (n=2-4) products were identified to have the hydroxysilylene structures  $HSiOH(H_2O)_n$  and the silica hydroxide structures  $SiOH(H_2O)_n$  (n=1-3), respectively. In particular, the  $HSiOH(H_2O)_n$  and  $SiOH(H_2O)_n$  (n=2 and 3) complexes were found to have cyclic hydrogen-bonded networks. Two possible pathways for the formation of the observed products have been discussed. This work provides new insights into the astrochemically relevant Si-O-H molecular architectures that are helpful for understanding the formation mechanism of cosmic particle.

Published under an exclusive license by AIP Publishing. https://doi.org/10.1063/5.0280490

# I. INTRODUCTION

The predominance of silicon, oxygen, and hydrogen as the second, first, and tenth most abundant elements in earth's crust, coupled with their higher cosmic abundances (ranked eighth, third, and first, respectively), has driven extensive research into the Si–O–H molecular systems.  $^{1-7}$  Studies of Si–O–H containing species help understand the microscopic mechanism of complicated processes of planetary surfaces and interstellar media.  $^{8.9}$  The insertion products HSiOH and HSiOH(H<sub>2</sub>O) were characterized from the matrixisolation infrared (IR) spectroscopic studies of the reactions of Si atoms with H<sub>2</sub>O.  $^{10}$  The stable existence of HSiOH and H<sub>2</sub>SiO in the gas phase was verified by neutralization–reionization mass spectrometric and theoretical studies.  $^{11-13}$  A tunable vacuum ultraviolet (VUV) photoionization crossed molecular beam study of the

reaction between atomic oxygen (O) and silane (SiH<sub>4</sub>) revealed the formation of the products of  $H_2SiOH$ , HSiOH, and SiOH. The rotational spectrum of the triatomic radical SiOH in the  $X^2A'$  ground state was measured in a supersonic molecular beam using Fourier transform microwave spectroscopy. Recently, the gas-phase HSiOH molecule has been identified by using laser-induced fluorescence spectroscopy. Theoretical studies of the  $H_2SiO/HSiOH$  and SiOH/HSiO systems provided a foundation for interpreting experimental spectra.  $^{2,17-28}$ 

In astrochemical research, the cationic reaction  $\mathrm{Si}^+ + \mathrm{H}_2\mathrm{O} \rightarrow \mathrm{SiOH}^+ + \mathrm{H}$  serves as a key pathway for removing  $\mathrm{Si}^+$  in earth's upper atmosphere (introduced via meteoroid ablation).  $^{9,29,30}$  Crossed molecular beam experiments combined with *ab initio* electronic structure calculations revealed that the reaction of SiH with  $\mathrm{H}_2\mathrm{O}$  could form the HSiO, SiO,  $\mathrm{H}_2\mathrm{SiO}$ , and HSiOH products.  $^{31}$ 

<sup>&</sup>lt;sup>3</sup>Hefei National Laboratory, Hefei 230088, China

a) Authors to whom correspondence should be addressed: gli@dicp.ac.cn and ljiang@dicp.ac.cn

Although the reaction of Si atom with one  $H_2O$  molecule has been well studied, the investigation of the Si +  $nH_2O$  (n > 1) reactions remains scarce. In this work, we prepared the  $SiO_nH_{2n}$  and  $SiO_nH_{2n-1}$  (n=2-4) complexes via the reactions of Si atoms with the  $H_2O$  molecules by using the laser-evaporation cluster source. These two series of products were determined to have the  $HSiOH(H_2O)_n$  and  $SiOH(H_2O)_n$  (n=1-3) structures by using the IR-VUV spectroscopy and quantum chemical calculations. The possible mechanisms for the formation of  $HSiOH(H_2O)_n$  and  $SiOH(H_2O)_n$  (n=1-3) have been proposed.

# II. EXPERIMENTAL AND COMPUTATIONAL METHODS

#### A. Experimental methods

The IR spectra of neutral  $SiO_nH_{2n}$  and  $SiO_nH_{2n-1}$  (n=2-4) complexes were measured by using the IR-VUV spectroscopic setup, the details of which have been provided previously, 32,33 and a brief description is given as follows: Neutral  $SiO_nH_{2n}$  and  $SiO_nH_{2n-1}$ (n = 2-4) complexes were produced via laser vaporization under supersonic expansion conditions with a 0.4% H<sub>2</sub>O/helium mixture (Fig. 1). A second-harmonic Nd:YAG laser (532 nm, InnoLas Spit-Light 400) with a pulse energy of 2 mJ was used to ablate a silicon metal target (purity 99.99%). The reactive gas was introduced via a Parker valve (Series 009) with a pulse width of 170 µs. The molecular beam passed through a 4-mm-diameter skimmer (Beam Dynamics, Model 50.8) and entered the ionization region, where threshold ionization occurred. The extraction plate of the reflectron time-of-flight mass spectrometer (TOF-MS) was applied with a +2950 V DC high voltage. Charged species were deflected from the molecular beam by the DC electric field of the extraction plate. The VUV laser was generated using an ArF excimer laser (Coherent, GAMLAS EX5A) with a wavelength of 193 nm.

The pulsed valve, 532 nm laser, and VUV laser were operated at a frequency of 20 Hz. Tunable IR laser pulses were operated at a repetition rate of 10 Hz and introduced ~160 ns prior to the VUV pulses. Depletion of the selected neutral cluster mass signal was detected when the IR laser resonantly excited vibrational transitions and induced vibrational predissociation. The IR spectra were

recorded by subtracting the mass spectral signals with and without IR laser irradiation (IR-on minus IR-off). The IR spectra of sizeselected neutral complexes were obtained by scanning the ion signal intensity as a function of IR wavelength, with a step size of 2 cm<sup>-1</sup>. Each IR wavelength point was averaged over 600 laser shots to record the spectra. The IR power dependence of the signal was measured to ensure that the predissociation yield remained linearly proportional to photon flux. The tunable IR laser beam was generated using a potassium titanyl phosphate (KTP)/potassium titanyl arsenate (KTA) optical parametric oscillator/amplifier system (OPO/OPA, LaserVision) pumped using a seeded Nd:YAG laser (Continuum Surelite EX). This system provided tunability over 700 to 7000 cm<sup>-1</sup> with a linewidth of 1 cm<sup>-1</sup>. The wavelength of the OPO laser output was calibrated using a commercial wavelength meter (HighFinesse GmbH, WS6-200 VIS IR). Note that the IR photons generated from our tabletop LaserVision system are insufficient for vibrational predissociation in the hydrogen-bonded O-D···O stretch vibrational region (2000-2400 cm<sup>-1</sup>); for the clusters studied here, the Si + D<sub>2</sub>O experiments have not been carried out. The intense and tunable infrared radiation source (i.e., infrared free electron laser) would be helpful for such deuterium-substitution experiments.

# **B.** Computational methods

The geometry optimizations and frequency calculations of  $SiO_nH_{2n}$  and  $SiO_nH_{2n-1}$  (n=2-4) were performed at the MP2/aug-cc-pVDZ level by using the Gaussian 16 package.<sup>34</sup> The structures of transition states were optimized by using the Berny algorithm. Intrinsic reaction coordinate calculations were carried out for all identified transition states to confirm their proper connections between the initial and final states. The relative energies and energy barriers at 0 K included zero-point vibrational energy corrections. To account for method-related systematic errors, harmonic vibrational frequencies were scaled by a factor of 0.959.<sup>35</sup> The resulting stick spectra were convoluted with Gaussian line shape functions using a full width at half maximum (FWHM) of  $10 \text{ cm}^{-1}$ .

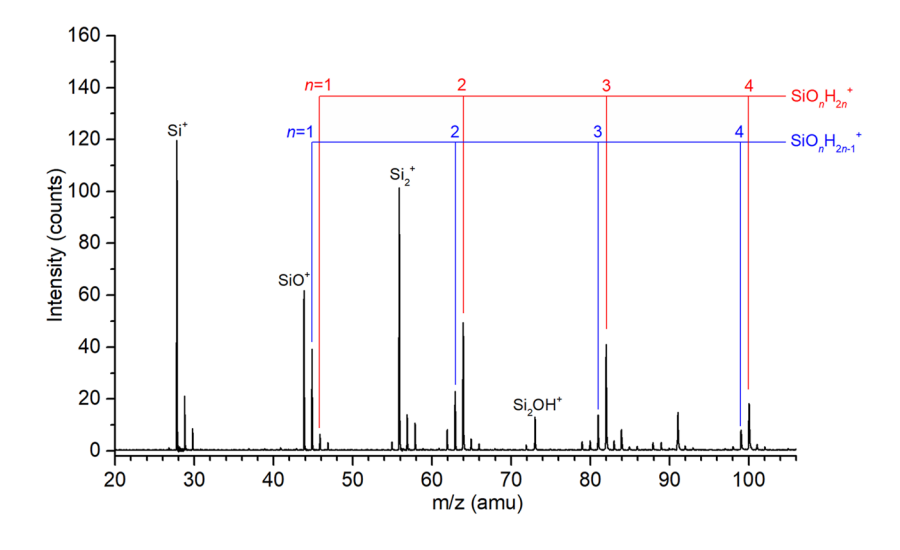


FIG. 1. VUV photoionization time-of-flight mass spectrum of the species formed from the reaction of Si atoms with  $H_2O$  molecules.

### **III. RESULTS AND DISSCUSION**

# A. Experimental infrared spectra

The experimental infrared spectra of  $SiO_nH_{2n}$  (n=2-4) in the OH stretching vibration region are shown in Figs. 2(a), 2(e), and 2(i), with the corresponding band positions listed in Table I. The

experimental spectrum of  $SiO_2H_4$  [Fig. 2(a)] exhibits three bands: band A (3696 cm<sup>-1</sup>), band B (3658 cm<sup>-1</sup>), and band C (3512 cm<sup>-1</sup>). The experimental spectrum of  $SiO_3H_6$  [Fig. 2(e)] contains four characteristic bands, which are centered at 3702 cm<sup>-1</sup> [labeled A(B)], 3674 cm<sup>-1</sup> (labeled C), 3299 cm<sup>-1</sup> (labeled D), and 3023 cm<sup>-1</sup> (labeled E). The experimental spectrum of  $SiO_4H_8$  [Fig. 2(i)] exhibits

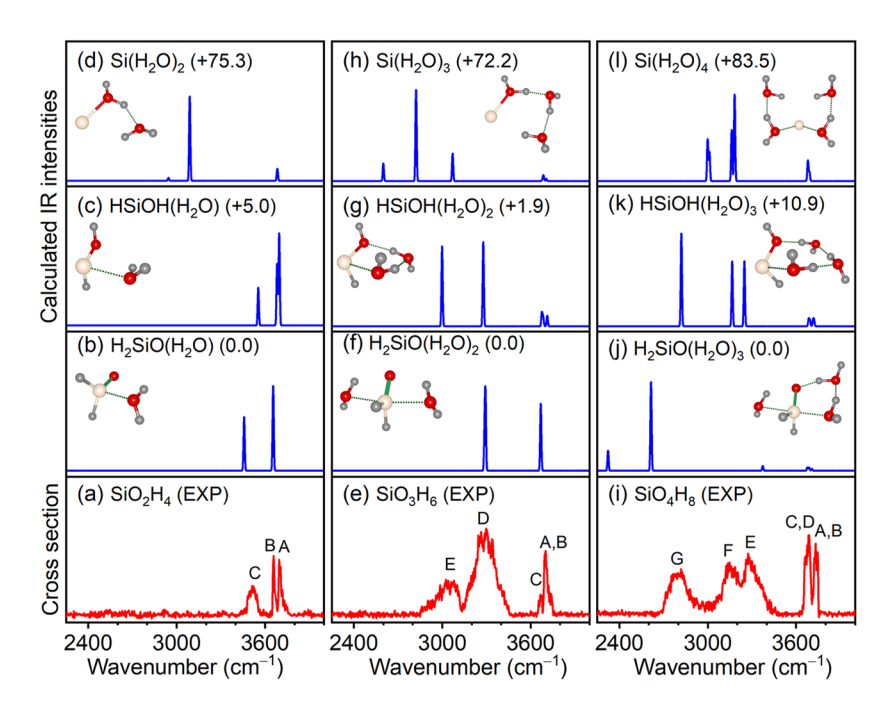


**FIG. 2.** Comparison of experimental IR spectra of neutral  $SiO_nH_{2n}$  (n=2-4) complexes [(a), (e), and (i)] and calculated IR spectra of the  $HSiOH(H_2O)_n$  (n=1-3),  $H_2SiO(H_2O)_n$  (n=1-3), and  $Si(H_2O)_n$  (n=2-4) isomers [(b)–(d), (f)–(h), and (j)–(l)]. Calculations were carried out at the MP2/aug-cc-pVDZ level of theory, with the harmonic vibrational frequencies scaled by a factor of 0.959. Relative energies (in parentheses) are listed in kcal/mol.

**TABLE I.** Comparison of the experimental band positions (cm<sup>-1</sup>) of neutral SiO<sub>n</sub>H<sub>2n</sub> (n = 2-4) complexes to the calculated values of HSiOH(H<sub>2</sub>O)<sub>n</sub> (n = 1-3) (isomers 1A–3A) obtained at the MP2/aug-cc-pVDZ level of theory (IR intensities are listed in parentheses in km/mol, and the calculated harmonic vibrational frequencies are scaled by a factor of 0.959).

Species	Isomer	Label	Exptl	Calcd	Mode
SiO <sub>2</sub> H <sub>4</sub>	HSiOH(H <sub>2</sub> O) (isomer 1A)	A	3696	3696(123)	Stretching mode of the O(1)H(1) group
		В	3658	3681(83)	Antisymmetric stretching modes of the $O(2)H(2)$ and $O(2)H(2')$ groups
		С	3512	3554(51)	Symmetric stretching modes of the O(2)H(2) and O(2)H(2') groups
SiO <sub>3</sub> H <sub>6</sub>	HSiOH(H <sub>2</sub> O) <sub>2</sub> (isomer 2A)	A	3702	3713(97)	Stretching mode of the O(3)H(3) group
		В		3686(86)	Stretching mode of the $O(1)H(1)$ group
		С	3674	3677(123)	Stretching mode of the O(2)H(2) group
		D	3299	3278(769)	Stretching mode of the O(3)H(3') group
		E	3023	2998(730)	Stretching mode of the O(2)H(2') group
SiO <sub>4</sub> H <sub>8</sub>	HSiOH(H <sub>2</sub> O) <sub>3</sub> (isomer 3A)	A	3732	3721(89)	Stretching mode of the O(3)H(3) group
		В		3714(85)	Stretching mode of the O(4)H(4) group
		С	3686	3693(89)	Stretching mode of the $O(1)H(1)$ group
		D		3685(111)	Stretching mode of the O(2)H(2) group
		E	3273	3248(991)	Stretching mode of the $O(3)H(3')$ group
		F	3139	3165(990)	Stretching mode of the O(4)H(4') group
		G	2781	2821(1410)	Stretching mode of the O(2)H(2') group

five distinct vibrational bands: band A(B) at 3732 cm $^{-1}$ , band C(D) at 3686 cm $^{-1}$ , band E at 3273 cm $^{-1}$ , band F at 3139 cm $^{-1}$ , and band G at 2781 cm $^{-1}$ . The observation of broad features in the 2700–3300 cm $^{-1}$  region in the SiO<sub>3</sub>H<sub>6</sub> and SiO<sub>4</sub>H<sub>8</sub> complexes implies the formation of hydrogen bonds.

As illustrated in Figs. 3(a), 3(e), and 3(i), analogous to the experimental IR spectra of  $SiO_nH_{2n}$  (n=2-4), the  $SiO_nH_{2n-1}$ 

(n = 2-4) complexes exhibit three, four, and five bands, respectively. The corresponding experimental frequencies are given in Table II.

# B. Identification of geometric structures

To interpret the experimentally observed spectral features and identify the structures of the  $SiO_nH_{2n}$  and  $SiO_nH_{2n-1}$  (n = 2-4)

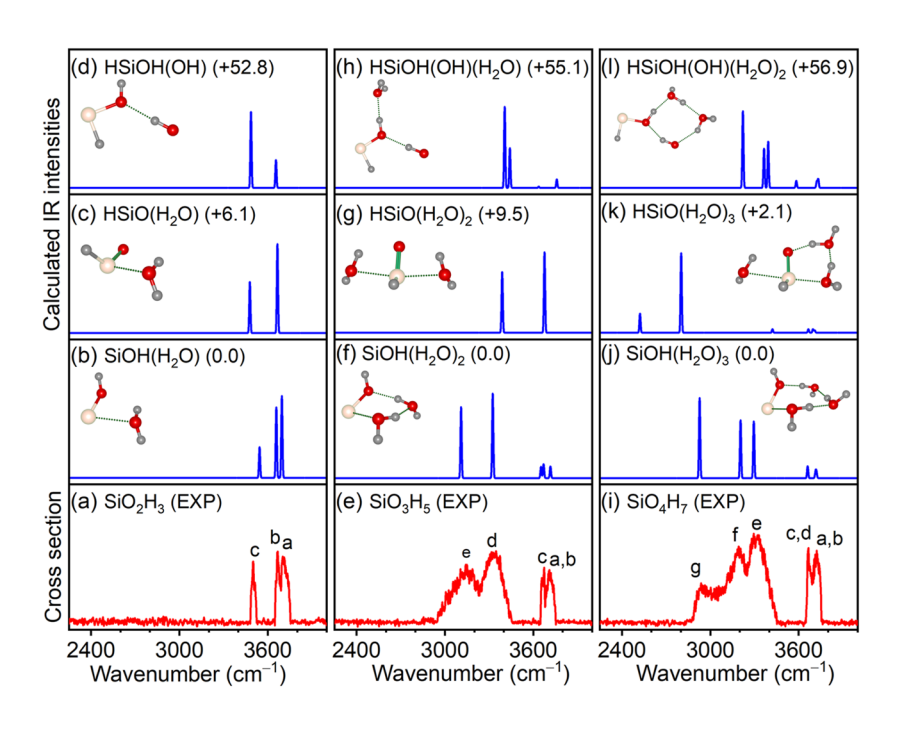
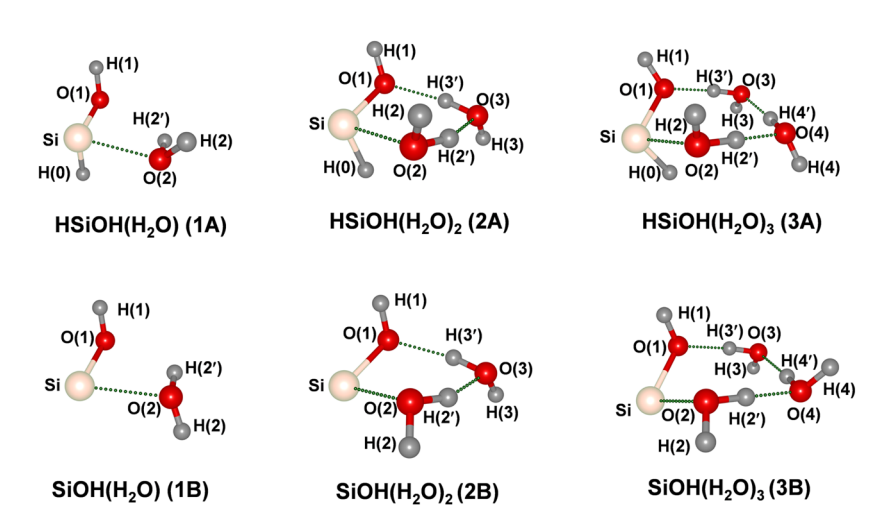


FIG. 3. Comparison of experimental IR spectra of neutral  $SiO_nH_{2n-1}$  (n=2-4) complexes [(a), (e), and (i)] and calculated IR spectra of the  $SiOH(H_2O)_n$  (n=1-3),  $HSiO(H_2O)_n$  (n=1-3), and HSiOH(OH) ( $H_2O)_m$  (m=0-2) isomers [(b)–(d), (f)–(h), and (j)–(l)]. Calculations were carried out at the MP2/aug-cc-pVDZ level of theory, with the harmonic vibrational frequencies scaled by a factor of 0.959. Relative energies (in parentheses) are listed in kcal/mol.

**TABLE II.** Comparison of the experimental band positions (cm $^{-1}$ ) of neutral SiO<sub>n</sub>H<sub>2n-1</sub> (n = 2-4) complexes to the calculated values of SiOH(H<sub>2</sub>O)<sub>n</sub> (n = 1-3) (isomers 1–3B) obtained at the MP2/aug-cc-pVDZ level of theory (IR intensities are listed in parentheses in km/mol, and the calculated harmonic vibrational frequencies are scaled by a factor of 0.959).

Species	Isomer	Label	Exptl	Calcd	Mode
SiO <sub>2</sub> H <sub>3</sub>	SiOH(H <sub>2</sub> O) (isomer 1B)	a	3702	3695(120)	Stretching mode of the O(1)H(1) group
		b	3668	3658(103)	Antisymmetric stretching modes of the $O(2)H(2)$ and $O(2)H(2')$ groups
		С	3500	3544(45)	Symmetric stretching modes of the O(2)H(2) and O(2)H(2') groups
SiO <sub>3</sub> H <sub>5</sub>	SiOH(H <sub>2</sub> O) <sub>2</sub> (isomer 2B)	a	3710	3717(98)	Stretching mode of the O(3)H(3) group
		b	3674	3670(117)	Stretching mode of the O(1)H(1) group
		С		3653(95)	Stretching mode of the O(2)H(2) group
		d	3325	3324(713)	Stretching mode of the O(3)H(3') group
		e	3105	3109(400)	Stretching mode of the O(2)H(2') group
SiO <sub>4</sub> H <sub>7</sub>	SiOH(H <sub>2</sub> O) <sub>3</sub> (isomer 3B)	a	3722	3720(88)	Stretching mode of the O(3)H(3) group
		b		3714(91)	Stretching mode of the O(4)H(4) group
		c	3666	3661(130)	Stretching mode of the $O(1)H(1)$ group
		d		3660(54)	Stretching mode of the O(2)H(2) group
		e	3295	3295(869)	Stretching mode of the O(3)H(3') group
		f	3191	3205(887)	Stretching mode of the O(4)H(4') group
		g	2937	2927(1230)	Stretching mode of the O(2)H(2') group



**FIG. 4.** Identified structures of neutral HSiOH( $H_2O$ ) $_n$  (n=1–3) (isomers 1A–3A) and SiOH( $H_2O$ ) $_n$  (n=1–3) (isomers 1B–3B) complexes (O, red; H, light gray; Si, light yellow). The atoms are labeled for discussion.

complexes, quantum chemical calculations were performed at the MP2/aug-cc-pVDZ level of theory. Three types of structures were localized for each cluster of  $SiO_nH_{2n}$  and  $SiO_nH_{2n-1}$ , respectively. The optimized structures and their simulated IR spectra of  $SiO_nH_{2n}$  and  $SiO_nH_{2n-1}$  are depicted in Figs. 2 and 3, respectively. The identified structures are shown in Fig. 4. The calculated band positions of identified structures are listed in Tables I and II, respectively.

# 1. $SiO_nH_{2n}$ (n = 2-4)

The most stable isomers of  $SiO_nH_{2n}$  (n=2-4) are predicted to have the  $H_2SiO(H_2O)_n$  (n=1-3) structures with a singlet ground state (Fig. 2), where the water molecules form weak bonds with the Si or O atoms. The next energetically higher isomers have the  $HSiOH(H_2O)_n$  (n=1-3) structures with an insertion-type HSiOH motif, which lie above the most stable isomers by 5.0, 1.9, and 10.9 kcal/mol for n=1, 2, and 3, respectively. The hydrated structures  $Si(H_2O)_n$  (n=2-4) are much higher in energy than the most stable isomers by 75.3, 72.2, and 83.5 kcal/mol for n=1, 2, and 3, respectively.

As shown in Fig. 2, only the simulated IR spectra of the  $HSiOH(H_2O)_n$  (n = 1-3) isomers exhibit the best agreement with the experimental spectra. In the simulated spectrum of HSiOH(H2O) [Fig. 2(c)], the calculated band at 3696 cm<sup>-1</sup> is attributed to the stretching mode of the O(1)H(1) group, which coincides with the experimental band A (3696 cm<sup>-1</sup>; Table I); the calculated bands at 3681 and 3554 cm<sup>-1</sup> are assigned to antisymmetric and symmetric stretching modes of the O(2)H(2) and O(2)H(2') groups, respectively, which are consistent with the experimental band B (3658 cm<sup>-1</sup>) and band C (3512 cm<sup>-1</sup>). In the calculated IR spectrum of HSiOH(H2O)2 [Fig. 2(g)], the stretching modes of the O(3)H(3) and O(2)H(2) groups were calculated to be 3713 and 3686 cm<sup>-1</sup>, respectively, which are close to the experimental band A(B) (3702 cm<sup>-1</sup>); the band at 3677 cm<sup>-1</sup> is attributed to the stretching mode of the O(1)H(1) group, which aligns with the experimental band C (3674 cm<sup>-1</sup>); the simulated bands at 3278 and 2998 cm<sup>-1</sup>, located within the hydrogen-bonding region, are attributed to the stretching modes of the O(3)H(3') and O(2)H(2')groups, respectively, which are consistent with the experimental band D (3299 cm $^{-1}$ ) and band E (3023 cm $^{-1}$ ). In the simulated spectrum of HSiOH(H<sub>2</sub>O)<sub>3</sub> [Fig. 2(k)], the bands at 3721 and 3714 cm $^{-1}$  are due to the stretching modes of the O(3)H(3) and O(4)H(4) groups, respectively, merging into a single composite band in the experimental spectrum [3732 cm $^{-1}$ , labeled A(B)]; the calculated bands at 3696 and 3685 cm $^{-1}$  are assigned to the stretching modes of the O(1)H(1) and O(2)H(2) groups, respectively, which are observed at the experimental band C(D) (3686 cm $^{-1}$ ); with increased hydrogen bonding, three stretching modes emerge in the hydrogen-bonding region: O(3)H(3'), O(4)H(4'), and O(2)H(2'), which are calculated to be 3248, 3165, and 2821 cm $^{-1}$ , respectively, in accordance with the experimental band E (3273 cm $^{-1}$ ), band F (3139 cm $^{-1}$ ), and band G (2781 cm $^{-1}$ ).

Furthermore, several theoretical methods were employed to systematically evaluate the relative stability of HSiOH(H2O) vs H<sub>2</sub>SiO(H<sub>2</sub>O), and the results are given in Table S1. It indicates that all the employed methods (i.e., B2PLYPD3, B3LYP(GD3), CCSD(T), MP4, etc.) predict HSiOH(H<sub>2</sub>O) to be at least 1.2 kcal/mol less stable than  $H_2SiO(H_2O)$ . The barrier for the conversion of  $HSiOH(H_2O)$ to H<sub>2</sub>SiO(H<sub>2</sub>O) is more than 56.1 kcal/mol, which might be sufficiently large so that the HSiOH(H2O) isomer could be kinetically trapped by the soft helium expansion of cold molecular beam prior to its rearrangement to the global minimum-energy structure  $H_2SiO(H_2O)$ . A thorough theoretical study of the  $Si + H_2O$  reaction showed that the barrier for the isomerization from HSiOH to H<sub>2</sub>SiO is very high (69.5 kcal/mol at the MP3/6-31G(d)//HF/6-31G(d) level of theory).<sup>18</sup> Indeed, HSiOH was observed in the Si + H<sub>2</sub>O reaction, with the absence of H<sub>2</sub>SiO.<sup>10</sup> Analogously, the previous matrix-isolation IR spectroscopy study indicated that the HSiOH(H2O) cluster is preferentially formed under water-excess conditions.<sup>10</sup> However, the microwave spectroscopic study of glow discharge of the SiH<sub>4</sub> + O<sub>2</sub> + Ar mixture identified H<sub>2</sub>SiO rather than HSiOH,<sup>21</sup> indicative of a different reaction mechanism as compared to the Si + H<sub>2</sub>O reaction. As shown in Fig. S2, even though the simulated IR spectra of H<sub>2</sub>SiO(H<sub>2</sub>O) and H<sub>2</sub>SiO(H<sub>2</sub>O)<sub>2</sub> seem to match the part of experimental IR spectra, the simulated IR spectrum of H<sub>2</sub>SiO(H<sub>2</sub>O)<sub>3</sub> is remarkably different from the experimental one, indicating that the  $H_2SiO(H_2O)_n$  (n = 1-3) isomers do not contribute to the experimental spectra. The absence of  $H_2SiO(H_2O)_n$  (n=1-3) could be due to the lack of the  $H_2SiO$  precursor in the Si +  $H_2O$  gas-phase reaction, which is reminiscent of the observation of the energetically higher isomers  $OTiCCO(CO)_n$  rather than the global-minimum  $Ti(CO)_n$  (n=6 and 7).<sup>36</sup> The extremely-high lying  $Si(H_2O)_n$  (n=2-4) isomers can also be ruled out by the discrepancy of simulated IR spectra from the experimental ones. The agreement of the simulated IR spectra of the  $HSiOH(H_2O)_n$  (n=1-3) isomers with the experimental ones is reasonable to confirm the assignment of these isomers as responsible for  $SiO_nH_{2n}$  (n=2-4).

# 2. $SiO_nH_{2n-1}$ (n = 2-4)

As shown in Fig. 3, the lowest-energy isomers of the  $SiO_nH_{2n-1}$  complexes adopt the silica hydroxide  $SiOH(H_2O)_n$  structures. The  $HSiO(H_2O)_n$  isomers lie slightly higher in energy than the  $SiOH(H_2O)_n$  isomers by 6.1 (n=1), 9.8 (n=2), and 2.0 (n=3) kcal/mol, respectively. The HSiOH(OH)  $(H_2O)_m$  isomers are significantly less stable than the  $SiOH(H_2O)_n$  isomers by 52.8 (m=0), 55.1 (m=1), and 56.9 (m=2) kcal/mol, respectively. Previous theoretical study has also demonstrated that SiOH exhibits greater thermodynamic stability than  $HSiO.^{37}$  Analogously, the  $SiOH^+$  isomer is also much more stable than the  $HSiO^+$  isomer. SiOH $^+$  does not undergo proton transfer with  $H_2O$  but rather forms the hydrated complex  $SiOH(H_2O)^+$ . 30

As illustrated in Fig. 3, the simulated IR spectra of the  $SiOH(H_2O)_n$  (n=1-3) isomers agree best with the experimental spectra. For the  $SiOH(H_2O)$  isomer, the antisymmetric and symmetric stretching vibrations of the O(2)H(2) and O(2)H(2') groups at 3695 and 3544 cm<sup>-1</sup> (Table II) align with the experimental band a (3702 cm<sup>-1</sup>) and band c (3500 cm<sup>-1</sup>), respectively; the O(1)H(1) stretching mode at 3658 cm<sup>-1</sup> agrees with the experimental band b (3668 cm<sup>-1</sup>). For the  $SiOH(H_2O)_2$  isomer, the O(3)H(3) stretching vibration at 3717 cm<sup>-1</sup> matches the

experimental band a (3710 cm<sup>-1</sup>); the stretching modes of the O(2)H(2) and O(1)H(1) groups at 3670 and 3653 cm<sup>-1</sup> are consistent with the experimental band b(c) (3674 cm<sup>-1</sup>); the stretching vibrations of the O(3)H(3') and O(2)H(2') groups at 3324 and  $3109~\text{cm}^{-1}$  agree well with the experimental band d (3325  $\text{cm}^{-1}$ ) and band e (3105 cm<sup>-1</sup>). For the SiOH(H<sub>2</sub>O)<sub>3</sub> isomer, the stretching modes of the O(4)H(4) and O(3)H(3) groups at 3720 and 3714 cm<sup>-</sup> merge into one experimental band a(b) (3722 cm<sup>-1</sup>); the nearly degenerate O(1)H(1) and O(2)H(2) stretching frequencies at 3661 and 3660 cm<sup>-1</sup> map to the experimental band c(d) (3666 cm<sup>-1</sup>); the stretching modes of the O(4)H(4') (3295 cm<sup>-1</sup>), O(3)H(3') $(3205 \text{ cm}^{-1})$ , and O(2)H(2')  $(2927 \text{ cm}^{-1})$  groups closely match the experimental band e (3295 cm<sup>-1</sup>), band f (3191 cm<sup>-1</sup>), and band g (2937 cm<sup>-1</sup>). In the simulated IR spectrum of the HSiO(H<sub>2</sub>O)<sub>3</sub> isomer [Fig. 3(k)], the 2522 cm<sup>-1</sup> band is not observed experimentally. It thus appears that the  $HSiO(H_2O)_n$  isomers do not contribute to the experimental spectra. The  $HSiOH(OH)(H_2O)_m$  isomers may lie too high in energy to be probed in the experiment.

### C. Formation mechanism

The  $HSiOH(H_2O)_n$  and  $SiOH(H_2O)_n$  (n=1–3) complexes represent two distinct product categories formed from the reactions of the Si atoms with the water molecules. Quantum chemical calculations were performed at the MP2/aug-cc-pVDZ level to understand the formation mechanism of these products. Potential energy profiles of reaction pathways are shown in Figs. 5 and S1, respectively. Thermodynamic data of relevant reactions are listed in Table S2.

As illustrated in Fig. 5, the reaction of a Si atom with one  $\rm H_2O$  molecule to produce IM1 [Si( $\rm H_2O$ )] is predicted to be exothermic by 14.8 kcal/mol. The following reactions are critical for generating the observed products:

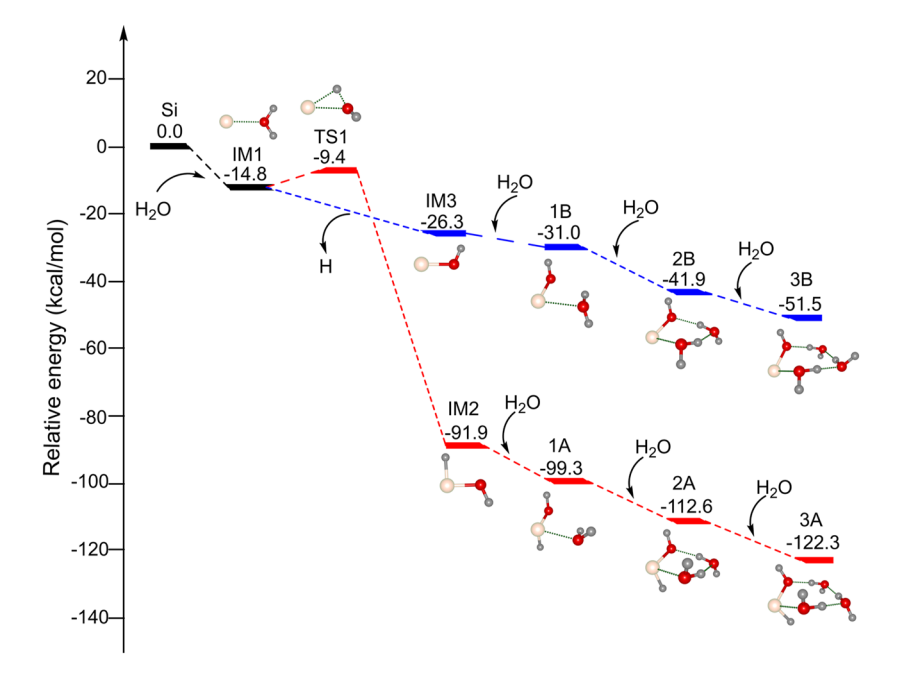


**FIG. 5.** Potential energy profiles of path A (red line) for the formation of HSiOH(H<sub>2</sub>O)<sub>n</sub> (n=1–3) (isomers 1A–3A) and path B (blue line) for the formation of SiOH(H<sub>2</sub>O)<sub>n</sub> (n=1–3) (isomers 1B–3B) calculated at the MP2/aug-cc-pVDZ level of theory. The abbreviation "IM" stands for intermediate and "TS" for transition state. The corresponding structures are embedded in the inset (O, red; H, light gray; Si, light yellow).

$$Si(H_2O) \rightarrow HSiOH,$$
 (1)

$$Si(H_2O) \rightarrow SiOH + H.$$
 (2)

In path A (red line), the isomerization from IM1 [Si(H<sub>2</sub>O)] to IM2 [HSiOH] [reaction (1)] is extremely exothermic by 77.1 kcal/mol via a transition state (TS1) with a small barrier of 9.4 kcal/mol. IM2 [HSiOH] reacts with H<sub>2</sub>O to form isomer 1A [HSiOH(H<sub>2</sub>O)] (exothermic by 7.3 kcal/mol). Subsequent H<sub>2</sub>O addition to isomer 1A yields isomer 2A [HSiOH(H<sub>2</sub>O)<sub>2</sub>] (exothermic by 13.3 kcal/mol) and isomer 3A [HSiOH(H2O)3] (exothermic by 9.7 kcal/mol), respectively.

In path B (blue line), the  $Si(H_2O) \rightarrow SiOH + H$  process [reaction (2)] is exothermic by 11.5 kcal/mol and kinetically feasible under laser ablation conditions.  $^{38,39}$  The  $Si^+ + H_2O \rightarrow SiOH^+ + H$ pathway was also facile in the ion reaction studies.<sup>29,30</sup> Analogous to path A, IM3 [SiOH] reacts with H2O to generate isomer 1B [SiOH(H<sub>2</sub>O)] (exothermic by 4.7 kcal/mol), which further combines with water molecules to form isomer 2B [SiOH(H2O)2] (exothermic by 10.9 kcal/mol) and isomer 3B [SiOH(H<sub>2</sub>O)<sub>3</sub>] (exothermic by 9.6 kcal/mol), respectively.

As shown in Fig. S1, IM1 [Si(H2O)] may react with a second H<sub>2</sub>O molecule to produce IM4 [(Si(H<sub>2</sub>O)<sub>2</sub>)], which is exothermic by 9.0 kcal/mol. Similarly, in path A (red line), IM4 [(Si(H<sub>2</sub>O)<sub>2</sub>)] could undergo isomerization to generate isomer 1A [HSiOH(H2O)] via reaction (3), which releases 75.5 kcal/mol energy with a 3.3 kcal/mol barrier (TS2),

$$Si(H_2O)_2 \rightarrow HSiOH(H_2O),$$
 (3)

$$Si(H_2O)_2 \rightarrow SiOH(H_2O) + H.$$
 (4)

Subsequent hydration steps yield isomer 2A [HSiOH(H<sub>2</sub>O)<sub>2</sub>] (exothermic by 13.3) and isomer 3A [HSiOH(H2O)3] (exothermic by 9.7 kcal/mol), respectively. In path B (blue line), reaction (4) is predicted to be exothermic by 7.2 kcal/mol, initiating the formation of SiOH(H<sub>2</sub>O)<sub>n</sub> (n = 1-3) complexes. Further hydration of isomer 1B [SiOH(H<sub>2</sub>O)] produces isomer 2B [SiOH(H<sub>2</sub>O)<sub>2</sub>] (exothermic by 10.9 kcal/mol) and isomer 3B [SiOH(H<sub>2</sub>O)<sub>3</sub>] (exothermic by 9.6 kcal/mol), respectively. Both pathways A and B are found to be thermodynamically exothermic and kinetically feasible.

# IV. CONCLUSION

We synthesized and structurally characterized neutral  $SiO_nH_{2n}$ and  $SiO_nH_{2n-1}$  (n = 2-4) complexes in the gas phase using sizespecific IR-VUV spectroscopy and quantum chemical calculations. Two distinct types of products,  $HSiOH(H_2O)_n$  and  $SiOH(H_2O)_n$ (n = 1-3), have been observed, enriching the characterization of novel astrochemically relevant Si-O-H molecular architectures. Systematic exploration of the Si + H2O potential energy surfaces revealed that the formation of these products is both thermodynamically exothermic and kinetically facile in the gas phase. The absence of  $H_2SiO(H_2O)_n$  (n = 1-3) could be due to the lack of the H<sub>2</sub>SiO precursor in the gas-phase reaction of Si atoms with water. These findings advance fundamental understanding of metal-water reactions and provide mechanistic insights into cosmic silicate particle formation through interstellar silicon-water interactions.

#### SUPPLEMENTARY MATERIAL

The supplementary material encompasses potential energy profiles of the formation of  $HSiOH(H_2O)_n$  and  $SiOH(H_2O)_n$ , relative energies of HSiOH(H2O) as compared to H2SiO(H2O), reaction energies of the formation of  $HSiOH(H_2O)_n$  and  $SiOH(H_2O)_n$ , and Cartesian coordinates of the structures.

#### **ACKNOWLEDGMENTS**

The authors gratefully acknowledge the staff members of the Dalian Coherent Light Source (Grant No. 31127.02.DCLS) for technical support and assistance in data collection. This work was supported by the National Natural Science Foundation of China (Grant Nos. 22125303, 92361302, 22103082, 22273101, 22288201, and 21327901), the Strategic Priority Research Program of the Chinese Academy of Sciences (Grant No. XDB0970100), the National Key Research and Development Program of China (Grant No. 2021YFA1400501), the Innovation Program for Quantum Science and Technology (Grant No. 2021ZD0303304), Dalian Institute of Chemical Physics (Grant No. DICP I202437), Chinese Academy of Sciences (Grant No. GJJSTD20220001), and the International Partnership Program of CAS (Grant No. 121421KYSB20170012).

#### **AUTHOR DECLARATIONS**

#### **Conflict of Interest**

The authors have no conflicts to disclose.

# **Author Contributions**

Wenhui Yan: Data curation (equal); Formal analysis (equal); Investigation (equal); Methodology (equal); Writing - original draft (equal). Shuai Jiang: Data curation (equal); Formal analysis (equal); Investigation (equal). Shangdong Li: Methodology (equal); Resources (equal); Software (equal). Jianxing Zhuang: Investigation (equal); Validation (equal); Visualization (equal). Ailin Wang: Resources (equal); Software (equal); Visualization (equal). Hua Xie: Funding acquisition (equal); Supervision (equal); Visualization (equal). Gang Li: Conceptualization (equal); Funding acquisition (equal); Project administration (equal); Validation (equal); Writing - original draft (equal). Ling Jiang: Conceptualization (equal); Funding acquisition (equal); Project administration (equal); Supervision (equal); Validation (equal); Writing - original draft (equal); Writing - review & editing (equal).

# **DATA AVAILABILITY**

The data that support the findings of this study are available within the article and its supplementary material.

# **REFERENCES**

<sup>1</sup>M. D. Allendorf, C. F. Melius, P. Ho, and M. R. Zachariah, J. Phys. Chem. 99,

<sup>2</sup>R. V. Olkhov and O. Dopfer, Chem. Phys. Lett. 314, 215 (1999).

- <sup>3</sup>D. Ngo, H. Liu, Z. Chen, H. Kaya, T. J. Zimudzi, S. Gin, T. Mahadevan, J. Du, and S. H. Kim, npj Mater. Degrad. 4, 1 (2020).
- <sup>4</sup>A. A. de Donato, B. A. Ghejan, J. M. Bakker, T. M. Bernhardt, S. T. Bromley, and S. M. Lang, ACS Earth Space Chem. **8**, 1154 (2024).
- <sup>5</sup>Z. Pei, Z. Feng, Z. Yao, Y. Luo, and J. Lu, Mol. Catal. **570**, 114667 (2025).
- <sup>6</sup>F. X. Brown, S. Yamamoto, and S. Saito, J. Mol. Struct. **413**, 537 (1997).
- <sup>7</sup>M. Cypryk and J. Chojnowski, J. Organomet. Chem. **642**, 163 (2002).
- <sup>8</sup> J. L. Turner and A. Dalgarno, Astrophys. J. 213, 386 (1977).
- <sup>9</sup>E. E. Ferguson, D. W. Fahey, F. C. Fehsenfeld, and D. L. Albritton, Planet. Space Sci. 29, 307 (1981).
- <sup>10</sup> Z. K. Ismail, R. H. Hauge, L. Fredin, J. W. Kauffman, and J. L. Margrave, J. Chem. Phys. 77, 1617 (1982).
- <sup>11</sup>D. K. Bohme, S. Wlodek, and H. Wincel, J. Am. Chem. Soc. **113**, 6396 (1991).
- <sup>12</sup>R. Srinivas, J. Hrusak, D. Sulzle, D. K. Bohme, and H. Schwarz, J. Am. Chem. Soc. 114, 2802 (1992).
- <sup>13</sup>R. Srinivas, D. K. Bohme, D. Sulzle, and H. Schwarz, J. Phys. Chem. **95**, 9836 (1991).
- <sup>14</sup>C. Chaudhuri, I. C. Lu, J. J. Lin, and S. H. Lee, Chem. Phys. Lett. 444, 237 (2007).
- <sup>15</sup> M. C. McCarthy, F. Tamassia, D. E. Woon, and P. Thaddeus, J. Chem. Phys. 129, 184301 (2008).
- <sup>16</sup>T. J. Herman, F. X. Sunahori, T. C. Smith, and D. J. Clouthier, J. Chem. Phys. 162, 044301 (2025).
- <sup>17</sup>T. Kudo and S. Nagase, Chem. Phys. Lett. **128**, 507 (1986).
- <sup>18</sup>S. Sakai, M. S. Gordon, and K. D. Jordan, J. Phys. Chem. **92**, 7053 (1988).
- <sup>19</sup>Y. Xie and H. F. Schaefer, J. Chem. Phys. **93**, 1196 (1990).
- <sup>20</sup>C. L. Darling and H. B. Schlegel, J. Phys. Chem. **97**, 8207 (1993).
- <sup>21</sup> S. Bailleux, M. Bogey, C. Demuynck, J. L. Destombes, and A. Walters, J. Chem. Phys. **101**, 2729 (1994).
- <sup>22</sup>B. Ma, N. L. Allinger, and H. F. Schaefer, J. Chem. Phys. **105**, 5731 (1996).
- <sup>23</sup>H. C. Tandon and N. K. Ray, J. Mol. Struc.: THEOCHEM 367, 62 (1996).
- <sup>24</sup>Y. Yamaguchi, Y. Xie, S. J. Kim, and H. F. Schaefer, J. Chem. Phys. **105**, 1951 (1996).
- <sup>25</sup>J. M. L. Martin, J. Phys. Chem. A **102**, 1394 (1998).

- <sup>26</sup> J. Koput, Chem. Phys. Lett. **324**, 201 (2000).
- <sup>27</sup> J. Koput, J. Phys. Chem. A **106**, 12067 (2002).
- <sup>28</sup>T. Taketsugu, N. Watanabe, and K. Hirao, J. Chem. Phys. **111**, 3410 (1999).
- <sup>29</sup>S. Wlodek, A. Fox, and D. K. Bohme, J. Am. Chem. Soc. **109**, 6663 (1987).
- <sup>30</sup>D. W. Fahey, F. C. Fehsenfeld, E. E. Ferguson, and L. A. Viehland, J. Chem. Phys. 75, 669 (1981).
- <sup>31</sup> C. He, S. Doddipatla, Z. Yang, S. J. Goettl, R. I. Kaiser, V. N. Azyazov, A. M. Mebel, and T. J. Millar, Astrophys. J. Lett. 921, L7 (2021).
- <sup>32</sup>G. Li, C. Wang, Q. Li, H. Zheng, T. Wang, Y. Yu, M. Su, D. Yang, L. Shi, J. Yang, Z. He, H. Xie, H. Fan, W. Zhang, D. Dai, G. Wu, X. Yang, and L. Jiang, Rev. Sci. Instrum. 91, 034103 (2020).
- <sup>33</sup>G. Li, C. Wang, H. J. Zheng, T. T. Wang, H. Xie, X. M. Yang, and L. Jiang, Chin. J. Chem. Phys. **34**, 51 (2021).
- 34 M. J. Frisch, G. W. Trucks, H. B. Schlegel, G. E. Scuseria, M. A. Robb, J. R. Cheeseman, G. Scalmani, V. Barone, G. A. Petersson, H. Nakatsuji, X. Li, M. Caricato, A. V. Marenich, J. Bloino, B. G. Janesko, R. Gomperts, B. Mennucci, H. P. Hratchian, J. V. Ortiz, A. F. Izmaylov, J. L. Sonnenberg, D. Williams-Young, F. Ding, F. Lipparini, F. Egidi, J. Goings, B. Peng, A. Petrone, T. Henderson, D. Ranasinghe, V. G. Zakrzewski, J. Gao, N. Rega, G. Zheng, W. Liang, M. Hada, M. Ehara, K. Toyota, R. Fukuda, J. Hasegawa, M. Ishida, T. Nakajima, Y. Honda, O. Kitao, H. Nakai, T. Vreven, K. Throssell, J. A. Montgomery, Jr., J. E. Peralta, F. Ogliaro, M. J. Bearpark, J. J. Heyd, E. N. Brothers, K. N. Kudin, V. N. Staroverov, T. A. Keith, R. Kobayashi, J. Normand, K. Raghavachari, A. P. Rendell, J. C. Burant, S. S. Iyengar, J. Tomasi, M. Cossi, J. M. Millam, M. Klene, C. Adamo, R. Cammi, J. W. Ochterski, R. L. Martin, K. Morokuma, O. Farkas, J. B. Foresman, and D. J. Fox, *Gaussian 16 Revision B.01*, Gaussian, Inc., Wallingford, CT, 2016.
- <sup>35</sup>R. D. Johnson, NIST computational chemistry comparison and benchmark database, 2006, https://cccbdb.nist.gov.
- <sup>36</sup>C. Wang, Q. Li, X. Kong, H. Zheng, T. Wang, Y. Zhao, G. Li, H. Xie, J. Yang, G. Wu, W. Zhang, D. Dai, M. Zhou, X. Yang, and L. Jiang, J. Phys. Chem. Lett. 12, 1012 (2021).
- <sup>37</sup>G. Frenking and H. F. Schaefer, J. Chem. Phys. **82**, 4585 (1985).
- <sup>38</sup>J. J. Zhang, C. Mueck-Lichtenfeld, and A. Studer, Nature **619**, 506 (2023).
- <sup>39</sup>S. Suzer and L. Andrews, J. Chem. Phys. **88**, 916 (1988).